PAPER ID: 1161
DOI: 10.18462/iir.rankine.2020.1161

Fluid Selection for Small-Scale Rankine Cycle Plants: Can You Draw Some Lines in the Sand?

Martin T. WHITE, Abdulnaser I. SAYMA

Department of Mechanical Engineering and Aeronautics, City, University of London
London, EC1V 0HB, United Kingdom, martin.white@city.ac.uk

ABSTRACT

The aim of this paper is to define general guidelines for fluid and cycle selection for small-scale Rankine cycle power systems based on heat-source temperature, heat-source temperature drop and heat sink availability. This is developed through optimisation studies for subcritical and supercritical cycles, which includes a model to estimate the achievable efficiency for a single-stage radial-inflow turbine, and the introduction of a fluid ranking procedure. The method is applied to 20 potential working fluids including hydrocarbons, hydrofluoroolefins, and siloxanes, alongside water, CO_2, Novec 649 and Novec 774. The results indicate that the top five working fluids are isobutane, isopentane, *n*-propane, R1233zd and *n*-pentane. Moreover, fluid selection is not significantly affected by heat-sink availability, whilst subcritical cycles are preferred for lower heat-source temperatures and heat-source temperature drops, whilst supercritical cycles are better for higher heat-source temperatures and are most suitable when trying to maximise power output.

Keywords: fluid selection; fluid classification; applications; thermodynamic optimisation

1. INTRODUCTION

Rankine cycles are widely investigated for converting low-temperature heat into electricity. Their various forms include subcritical and supercritical cycles, operating with an organic fluid, water, or carbon dioxide. The optimal pairing of cycle and fluid depends on maximising thermodynamic performance for the available heat source and heat sink, but also on a large number of other considerations including component design aspects, operating pressures, and the complexity and cost of the system, alongside fluid characteristics such as toxicity, flammability, cost and environmental impact. To this end, working-fluid selection for Rankine cycles is repeatedly discussed within the literature (e.g., Badr et al., 1985; Chen et al., 2010; Rahbar et al., 2017).

The optimal fluid will also depend on the application. For example, in waste-heat recovery applications a large heat-source temperature drop is preferred to maximise the amount of heat reclaimed by the cycle. In this instance, the reduction, or even removal, of isothermal heat transfer in the evaporator helps to reduce exergy destruction within the heat-addition heat exchanger. On the other hand, for an application such as a solar-thermal system, it is preferential to have a small heat-source temperature drop, to facilitate a higher average temperature of heat addition and thus obtain higher thermal efficiency. In this instance, the isothermal heat transfer process can be advantageous. Thus, it does not follow that the optimal fluid for one application is the same as another, even if operating temperatures are similar. Moreover, the optimal fluid may also depend on the scale of the application. For a large-scale application, where it is possible to consider more complex component designs, such as a multi-stage axial turbine, it may be suitable to identify an optimal fluid assuming a fixed expander efficiency, assuming that an expander with that efficiency can be achieved in practice. However, for a small-scale system, where the turbine design may be constrained to a single-stage design to minimise costs, fluid selection, cycle optimisation and component design should be completed simultaneously.

Currently, many existing fluid selection studies have assumed fixed expander efficiencies, whilst the distinction between applications with a small or large heat-source temperature drop has not been made. Moreover, owing to on-going changes to regulations, it is important to revisit previous studies with an on-going revision to the list of fluid candidates. To this end, the focus of this paper is to attempt to provide clarity in terms of working fluid selection for small-scale applications for different heat-source temperatures, heat-source temperature drops, and heat-sink conditions, whilst considering both subcritical and supercritical cycles and accounting for the effect of cycle operating conditions on turbine efficiency.

2. METHODOLOGY

2.1. Thermodynamic modelling

The Rankine cycle is modelled as a recuperated cycle, with either subcritical or supercritical operation. The cycle is assumed to operate under steady-state conditions, whilst heat losses and pressure drops are neglected. The cycle analysis is completed by applying an energy and mass balance to each component and measuring performance in terms of the net-power output. The five cycle variables are the cycle condensation temperature T_1, reduced evaporation pressure p_r, amount of superheat ΔT_{sh}, non-dimensional heat-source temperature drop θ, and recuperator effectiveness ε. The reduced evaporation pressure is defined as $p_r = p_2/p_{\mathrm{cr}}$, where p_2 is the evaporation pressure and p_{cr} is the fluid critical pressure. Thus, $p_r < 1$ and $p_r > 1$ correspond to subcritical and supercritical operation respectively. The expander inlet temperature is found from:

$$T_3 = \begin{cases} T_{\mathrm{sat}} + \Delta T_{\mathrm{sh}} & \text{if } p_r < 1 \\ T_{\mathrm{cr}} + \Delta T_{\mathrm{sh}} & \text{otherwise} \end{cases} \qquad \text{Eq. (1)}$$

where T_{sat} is the saturation temperature at the expander inlet pressure, and T_{cr} is the fluid critical temperature. The non-dimensional heat-source temperature drop determines the heat-source outlet temperature from:

$$\theta = \frac{T_{\mathrm{hi}} - T_{\mathrm{ho}}}{T_{\mathrm{hi}} - T_{\mathrm{ci}}} \qquad \text{Eq. (2)}$$

where T_{hi} and T_{ho} are the heat-source inlet and outlet temperatures, and T_{ci} is the heat-sink inlet temperature. The pump is modelled with a fixed isentropic efficiency of 70%, whilst the expander is assumed to be a radial-inflow turbine. The turbine isentropic efficiency is estimated according to the isentropic volumetric expansion ratio across the turbine ($V_{r,s} = \rho_3/\rho_{4s}$) according to the method developed in White and Sayma (2019):

$$\eta_{\mathrm{t}} = \eta_{\mathrm{t,max}}(1.007 - 0.004615\, V_{r,\mathrm{s}}) \qquad \text{Eq. (3)}$$

where $\eta_{\mathrm{t,max}}$ = 0.89. Equation (3) is used in an attempt to restrict an optimisation from identifying thermodynamic cycles with large volumetric expansion ratios for which it may be difficult to design an efficient radial-inflow turbine. All heat-exchange processes are discretised and the pinch points within each heat exchanger are calculated. These are constrained to be above the minimum allowed pinch point of 10 K.

2.2. Optimisation and fluid ranking procedure

For defined heat-source and heat-sink conditions (i.e., fluid, $T, p, \dot{m}$), optimisation can be used to identify the optimal cycle and working fluid. For a defined working fluid, the optimal cycle is found by completing a single-objective optimisation using the GlobalSearch function (Mathworks, 2019) to identify the optimal values for the five cycle variables (see Table 1) that result in the highest net power output. The optimisation is repeated for each fluid and the fluids are ranked and given a score, ranging between 1 (best performing) and n (worst performing), where n is the number of fluids considered. The fluids considered are listed in Section 2.3. It is worth noting that cycles that maximise power may not be the optimal cycles when other performance indicators, such as heat-exchanger area, total investment cost or payback period are considered. However, the authors previous study suggested that the optimal working fluid is independent of whether maximising power output or minimising heat-exchanger area is the objective. Specifically, it was suggested that the optimal fluid can be identified from a single-objective optimisation based on power output, and then the preferred trade-off between power and cost can be met by adjusting the heat-exchanger pinch points (White and Sayma, 2019).

Table 1. Bounds for the optimisation variables

	T_1	p_r	ΔT_{sh}	θ	ε
Lower bound	288	0.1	0	0	0
Upper bound	373	5.0	200	1	1

2.3. Assumptions for the study

The models described can be applied to a range of heat-source and heat-sink conditions and optimal working fluids identified. The heat source is assumed to be air at a temperature ranging between 423 and 623 K, whilst the heat sink is assumed to be water at 288 K. Since only thermodynamic aspects are considered here, the optimal cycle is independent of the heat-source mass-flow rate, which is set to $\dot{m}_{\mathrm{h}}$ = 1 kg/s. However, the optimal cycle is dependent on the heat-capacity rate ratio, $\dot{m}_{\mathrm{c}} c_{p,\mathrm{c}} / \dot{m}_{\mathrm{h}} c_{p,\mathrm{h}}$, and thus two heat-sink mass-flow rates will be considered, namely $\dot{m}_{\mathrm{c}}$ = 1 and 100 kg/s. Since the specific-heat capacity of air and water at 1 bar are approximately 1 and 4.2 kJ/(kg K), the heat-capacity rate ratios for the two cases are thus 4.2 and 420 respectively. Finally, to evaluate how the heat-source temperature drop affects the optimal working fluid, four cases are considered. In the first case, the optimisation of heat-source temperature is unconstrained and θ is included within the optimisation. In the other three cases θ is fixed to a value of 0.1, 0.2 and 0.5 respectively. The fluids considered within this study are summarised in Table 2. No CFC, HCFC and HFC fluids have been included, owing to their negative environmental impact and imposed regulations restricting their use. Therefore, the considered fluids represent fluids that could feasibly be used within future ORC power systems, and include hydrocarbons, siloxanes and hydrofluoroolefins, alongside other common fluids including water, carbon dioxide and the Novec fluids. In summary, for each fluid, the optimisation is completed for each combination of heat-source temperature, heat-sink mass-flow rate and heat-source temperature drop. In total, this corresponds to a total of 40 optimisation studies per working fluid, and a total of 800 optimisation studies.

Table 2. Summary of working fluids considered within this study. Fluid types: HC (hydrocarbon); HFO (hydrofluoroolefin); SI (siloxane).

Fluid	Type	T_{cr} [K]	p_{cr} [bar]	w_{m} [g/mol]	T_{b} [K]	Fluid	Type	T_{cr} [K]	p_{cr} [bar]	w_{m} [g/mol]	T_{b} [K]
CO_2	-	304.1	73.8	44.0	194.5	Novec649	-	441.8	18.7	316.0	321.8
SF_6	-	318.7	37.5	146.1	209.5	isopentane	HC	460.4	33.8	72.1	300.6
propylene	HC	364.2	45.6	42.1	225.2	Novec774	-	468.4	17.1	366.1	346.8
R1234yf	HFO	367.9	33.8	114.0	243.4	*n*-pentane	HC	469.7	33.7	72.1	308.8
n-propane	HFC	369.9	42.5	44.1	230.7	cyclopentane	HC	511.7	45.7	70.1	322.0
R1234ze	HFO	382.5	36.3	114.0	253.9	MM	SI	518.7	19.4	162.4	373.0
cyclopropane	HC	398.3	55.8	42.1	-	benzene	HC	562.0	49.1	78.1	352.8
propyne	HC	402.4	56.3	40.1	247.7	MDM	SI	564.1	14.2	236.5	425.2
isobutane	HC	407.8	36.3	58.1	261.1	toluene	HC	591.8	41.3	92.1	383.3
R1233zd	HFO	438.8	35.7	130.5	291.1	water	-	647.1	220.6	18.0	372.8

3. RESULTS

Following the process outlined previously, each working fluid obtains a score (ranging between 1 and 20, where a lower score represents a higher fluid ranking) for each of the 40 case studies considered. It is then possible to evaluate the score distribution across all of the cases considered, as reported in Figure 1. It is observed that hydrocarbons appear to represent the best fluids considering performance across the full range of heat-source and heat-sink conditions. Specifically, the three best fluids are all hydrocarbons, namely isobutane, isopentane and *n*-propane, with mean scores of 3.93, 4.83 and 5.08 respectively. These fluids are followed by R1233zd, which is the first non-hydrocarbon fluid, which has a mean score of 5.75, and another two hydrocarbons (*n*-pentane: 5.83; cyclopentane: 6.30). Ultimately, these results reinforce previous studies that have identified these fluids as particularly suitable for ORC systems and report their use in commercial ORC systems (Colonna et al., 2015). It is also worth commenting that the thermodynamic behaviour of R1233zd is very similar to that of R245fa, and can be considered as a drop-in replacement for R245fa (Eyerer et al., 2016). Thus, the results reported in Figure 1 help to reinforce these previous findings.

The other fluids considered to be suitable fluids within the literature, particularly for higher-temperature applications (i.e., aromatics and siloxanes), do not obtain as low scores. Specifically, for MM, benzene, MDM and toluene the mean scores are 10.8, 9.08, 16.3 and 11.3 respectively. This may be attributed to their high critical temperatures, and high boiling temperatures (see Tab. 2), which lead to large cycle pressure ratios, and

large expander volumetric expansion ratios. Therefore, since the focus of this study is on small-scale systems, and it is assumed that expansion is obtained over a single-stage radial-inflow turbine, these large expansion ratios lead to a reduction in the turbine isentropic efficiency (Eq. 3). This may indicate that these fluids might perform better for a large-scale application where multi-stage expansion can be considered. It should however be noted that Eq. 3 was derived from data that only went up to volume ratios of 10, and thus the validity of extrapolating this relationship to larger volumetric expansion ratios requires further investigation.

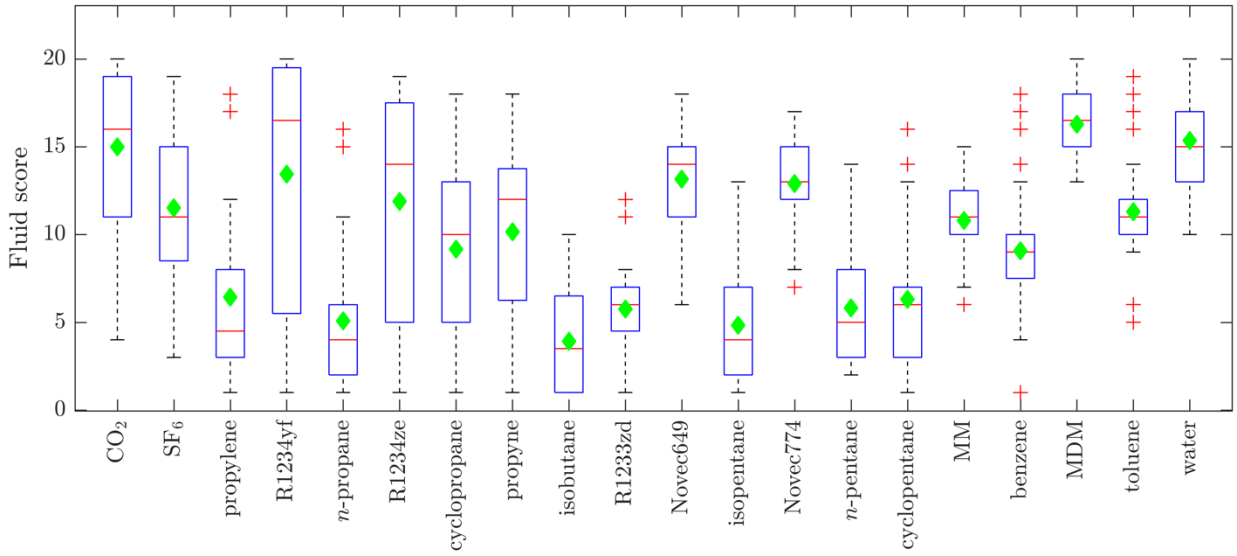

Figure 1. Boxplot showing the fluid score for each fluid, showing the mean (green diamond), median (horizontal red line), 25th and 75th percentiles (blue box), range (black dotted line) and outlines (red crosses).

It is also interesting to consider, for each working fluid and case study, whether the optimal cycle is a subcritical or supercritical cycle, as reported in Figure 2. The top plot reports the average score after the optimal cycles have been grouped into subcritical and supercritical cycles, whilst the bottom plot reports the number of times either cycle is identified. These results show a clear trend with supercritical cycles being preferred for fluids with lower critical temperatures, and subcritical cycles being preferred for fluids with higher critical temperatures. Specifically, the first five fluids are almost exclusively supercritical cycles (T_{cr} < 370 K), whilst all fluids from isopentane (T_{cr} > 460 K) onwards are subcritical cycles. The fluids in-between are hybrids and could be used in either a subcritical or supercritical cycle, depending on the application. Considering specific fluids, isobutane and R1233zd are the lowest scored supercritical cycles (3.00 and 4.00 respectively), whilst isopentane and *n*-pentane are the lowest scored subcritical cycles (4.69 and 6.30 respectively).

Each fluid can also be grouped, and the mean score obtained, according to the heat-source and heat-sink conditions. In Figure 3, the corresponding mean scores according to heat-sink mass-flow rate, heat-source temperature and heat-source temperature drop are reported. Considering the effect of the heat-sink, it is found that whilst fluids with lower critical temperatures perform slightly better for smaller heat sinks, and fluids with higher critical temperatures performance better for larger heat sinks, the optimal fluid selection is not strongly dependent on the relative size of the heat sink. Considering heat-source temperature, it is found that as T_{hi} increases, it becomes clearer which fluid is the optimal choice. For example, for T_{hi} = 423 K, the lowest score is 6.50 (isopentane), whilst for T_{hi} = 623 K the lowest mean score is 2.00 (*n*-propane). For the intermediate temperatures, isobutane obtains the lowest score, ranging between 3.00 and 2.88. This suggests that fluid selection is more critical for higher heat-source temperatures. Moreover, since the majority of the isopentane and *n*-propane cycles are subcritical and supercritical respectively, this suggests that subcritical cycles are preferred at lower heat-source temperatures, whilst supercritical cycles are preferred at higher temperatures.

Finally, it is found that the optimal fluids for non-dimensional heat-source temperature drops of 0.1, 0.2 and 0.5 are isopentane (2.6), isopentane (2.1) and *n*-propane (2.3), whilst propylene is the optimal fluid (2.6) for the maximum power cycles. This indicates that fluids with sufficiently high critical temperatures to allow subcritical cycles are preferred for applications with a low heat-source temperature drop. This is further evidenced by the relatively low scores obtained for *n*-pentane and cyclopentane for the θ = 0.1 and 0.2 cases.

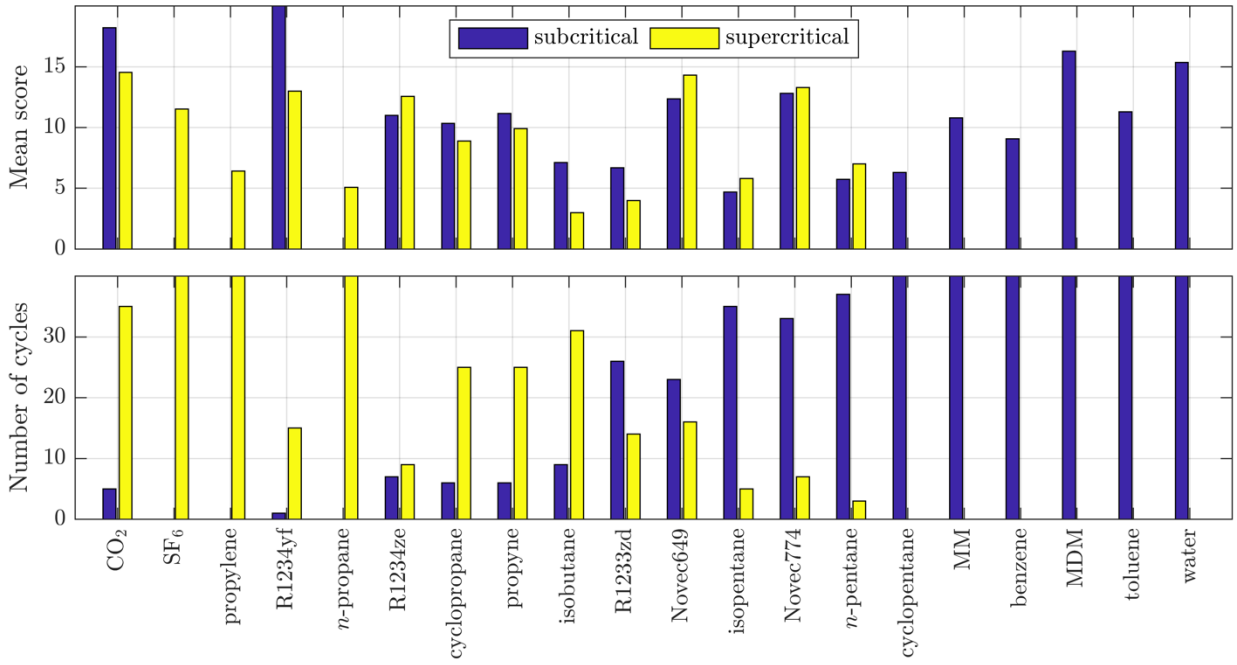

Figure 2. Average fluid score with results divided according to whether the optimal cycle is a subcritical or supercritical cycle (top), and number of subcritical and supercritical cycles identified for each fluid (bottom).

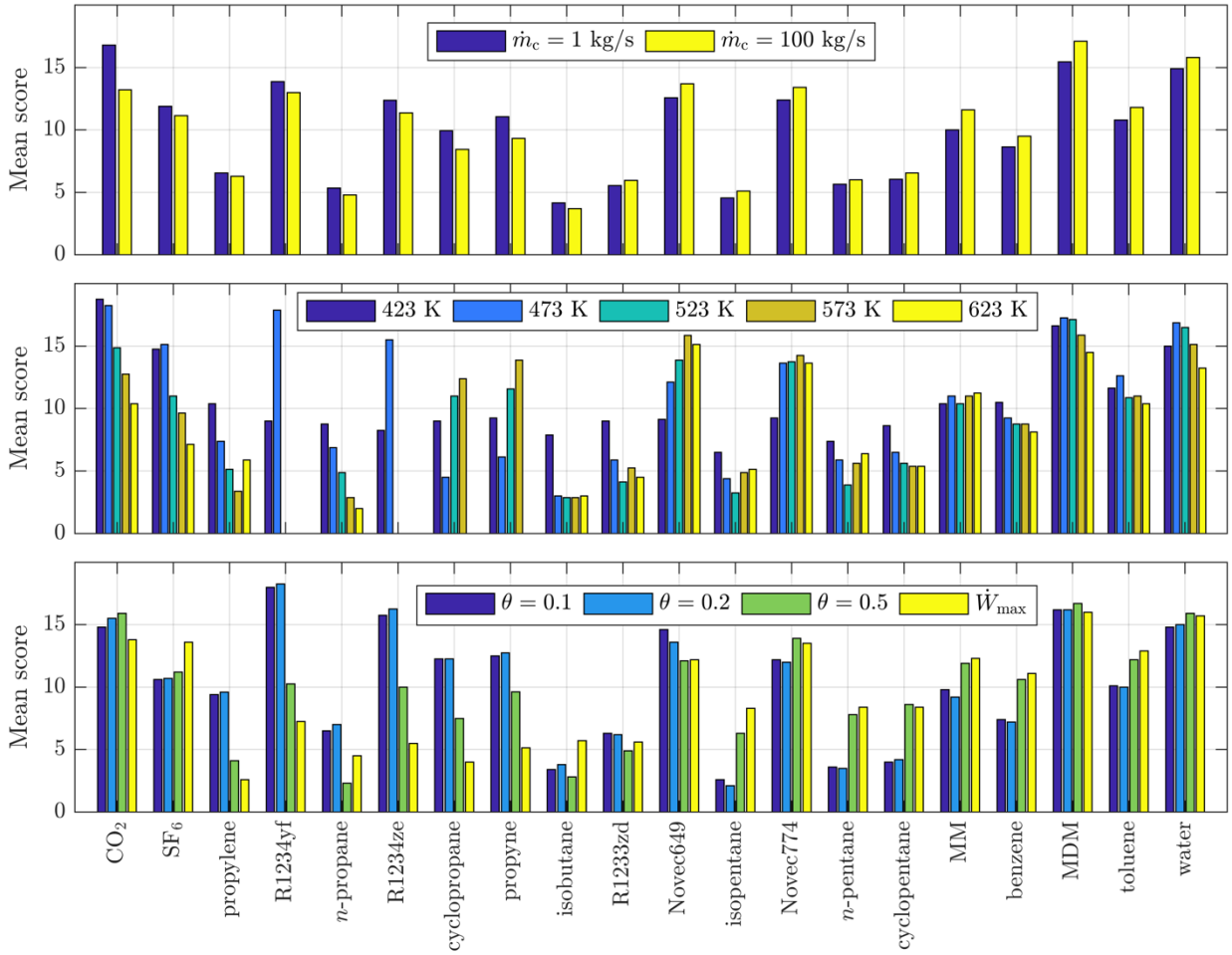

Figure 3. Average fluid score with results divided according to heat-sink mass-flow rate (top), heat-source temperature (middle) and non-dimensional heat-source temperature drop (bottom).

4. CONCLUSIONS

This paper has presented a parametric thermodynamic optimisation study to identify optimal working fluids and cycle architectures for small-scale Rankine cycle power systems for a range of different heat-source and heat-sink conditions. The results indicate that the top five working fluids, when considering performance over all of the case studies considered, are isobutane, isopentane, *n*-propane, R1233zd and *n*-pentane. When using isobutane and *n*-propane supercritical cycles are generally optimal, whilst subcritical cycles are generally preferred for isopentane and *n*-pentane. R1233zd can be used in both types of cycle. Moreover, it is found that fluid selection is not significantly affected by heat-sink availability, whilst subcritical cycles are preferred at lower heat-source temperatures, and low heat-source temperature drops, whilst supercritical cycles are better for higher heat-source temperatures and are most suitable when trying to maximise power output.

ACKNOWLEDGEMENTS

This work was supported by the UK Engineering and Physical Sciences Research Council (EPSRC) [grant number: EP/P009131/1].

NOMENCLATURE

$\dot{m}$	mass-flow rate (kg/s)
p	pressure (kPa)
p_r	reduced evaporation pressure
T	temperature (K)
$V_{r.s}$	volumetric expansion ratio (isentropic)
w_{m}	molecular weight (g/mol)
ε	recuperator effectiveness
η	isentropic efficiency
θ	heat-source temperature drop

Subscripts

1	pump inlet
2	pump outlet
3	expander inlet
b	boiling
c	heat-sink
ci	heat-sink inlet
cr	critical point
h	heat source
hi	heat-source inlet
ho	heat-source outlet
sat	saturation
t	turbine

REFERENCES

Badr, O., Probert, D., O'Callaghan, P.W., 1985. Selecting a working fluid for a Rankine-cycle engine. Applied Energy, 21(1), 1-42. doi:10.1016/0306-2619(85)90072-8.

Chen, H., Goaswami, D.Y., Stefanakos, E.K., 2010. A review of thermodynamic cycles and working fluids for the conversion of low-grade heat. Renew Sust Energy Rev, 14(9), 3059-3067. doi:10.1016/j.rser.2010.07.006.

Colonna, P., Casati, E., Trapp, C., Mathijssen, T., Larjola, J., Turunen-Saaresti, T., Uusitalo, A., 2015. Organic Rankine cycle power systems: from the concept to current technology, applications and an outlook to the future. J Eng Gas Turb Power, 137(10):100801. doi:10.1115/1.4029884.

Eyerer, S.,Wieland, C., Vandersickel, A., Spliethoff, H., 2016. Experimental study of an ORC (organic Rankine cycle) and analysis of R1233zd-E as a drop-in replacement for R245fa for low temperature heat utilization. Energy, 103, 660-671. doi:10.1016/j.energy.2016.03.034.

Mathworks, 2019. Global Optimization Toolbox: User's Guide (R2019b). The MathWorks, Inc, Natick, MA. Available: https://uk.mathworks.com/help/pdf_doc/gads/gads_tb.pdf [Accessed: 16th December 2019]

Rahbar, K., Mahmoud, S., Al-Dada, R.K., Moazami, N., Mirhadizadeh, S.A., 2017. Review of organic Rankine cycle for small-scale applications. Energy Conversion and Management, 134, 135-155. doi:10.1016/j.econman.2016.12.023.

White, M.T., Sayma, A.I., 2019. Simultaneous cycle optimization and fluid selection for ORC systems accounting for the effect of the operating conditions on turbine efficiency. Frontiers in Energy Research, 7(50). doi:10.3389/fenrg.2019.00050.